

EMI Suppression in Voltage Source Converters by Utilizing DC-link Decoupling Capacitors

Qian Liu, Shuo Wang, Carson Baisden, Fred Wang and Dushan Boroyevich
Center for Power Electronics Systems
The Bradley Department of Electrical and Computer Engineering
Virginia Polytechnic Institute and State University
Blacksburg, VA 24061 USA
Email: qiliu@vt.edu

Abstract— DC-link decoupling capacitors are normally used to control the voltage overshoot of switching devices in voltage source converters. This paper analyzes decoupling capacitors' impacts on device EMI noise as well as on device voltage stress. The design and selection of decoupling capacitors considering both voltage stress and EMI suppressions are presented. A new high-frequency EMI filter by utilizing the decoupling capacitors is proposed. The filter is adopted as a local EMI filter for power module. The integratable characteristics of the proposed filter are discussed. Simulation and experimental results verify the design. This high-frequency filter shows good attenuation for high-frequency EMI noise and voltage overshoot suppression.

Keywords: decoupling capacitor, Y capacitor, conducted EMI, EMI filter, common-mode (CM), differential-mode (DM), IPPEM

I. INTRODUCTION

The fast switching speed of semiconductor devices in power converters leads to self-inflicted voltage transients due to the stray parasitic inductance and capacitance in the converter [1-2]. In the state-of-the-art hard-switching voltage-source converters (VSCs), a DC-link decoupling capacitor is normally used to compensate the impact of the interconnect parasitics between DC bus and the device, and therefore reduce voltage stress on devices. Fig. 1 shows a typical three-phase voltage source inverter with all main parasitic inductances and the decoupling capacitor C_{dec} . The decoupling capacitor should be placed close to switching power modules. Compared with other device voltage overshoot suppression schemes such as active and passive snubbers, the decoupling capacitors are simpler, less lossy, and less expensive [3]. On the other hand, adding decoupling capacitors changes peak overshoot and device turn-on and turn-off transients, which in turn changes the conducted Electromagnetic Interference (EMI) noise frequency spectrum (150 KHz – 30 MHz) in a converter. The decoupling capacitors actually become an additional EMI noise propagation path.

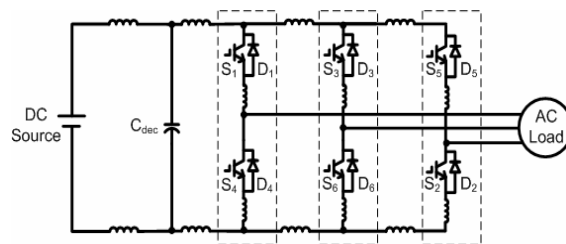


Fig. 1 Illustration of DC-link Decoupling Capacitor in VSC

In previous research [2], the voltage stress on device terminals in a VSC was studied. The amplitude of the voltage overshoot can be roughly predicted by knowing the device parasitic capacitance and the power circuit layout parasitic inductance. While one may take for granted that decoupling capacitors will help to reduce EMI noise, the selection of the decoupling capacitor with the consideration of both EMI noise and voltage overshoot is not fully explored. Previous research has not studied the effect of the decoupling capacitor on the converter EMI noise. The interactions among the decoupling capacitor, the rest of the noise propagation path, and the device module have not yet been characterized. Furthermore, from the standpoint of EMI noise attenuation, the EMI noise spectrum, including both noise frequency and magnitude, has also been altered when adding a decoupling capacitor. How to select the decoupling capacitor to help the input filter design has not been studied.

It is known that the device switching and its interaction with device module parasitics is the source of EMI noise in a power electronics converter [13]. The desire for containing the EMI noise within the switching module is a main motivation to study the effect of decoupling capacitor on EMI noise. The future trend of power electronics is integration of various functions in an electronic power processing module, including filtering functions [4]. Research has been carried out to integrate the decoupling capacitor into an Integrated Power Electronics Module (IPEM) [5-6] to reduce the voltage stress. Since EMI and its mitigation will be one of the determining future shaping factors for power processing, further research is desirable to contain EMI noise in the IPEM by designing and integrating the filtering components,

In this paper, the impact of decoupling capacitors on device voltage stress and EMI noise are analyzed together. The capacitance selection strategy based on balancing the need of suppressing both overshoot voltage and EMI noise is presented. A new method – a local filter close to the device module – for effective EMI filtering and stress control is proposed. The design and integration of the local filter during the device module packaging process is discussed. An IGBT-based chopper circuit is used to verify the analysis and filter design. The experimental results show that the proposed high-frequency EMI filter by utilizing the decoupling capacitors can have good attenuation for high-frequency EMI noise and voltage overshoot suppression.

II. ANALYSIS OF VOLTAGE STRESS AND EMI NOISE IMPACT OF DECOUPLING CAPACITORS

In order to operate devices safely, decoupling capacitors are usually used on the DC-link in hard-switching VSCs. The basic function of the capacitors, placed between the device module and the rest of the circuit, is to minimize the voltage overshoot due to the abrupt current change in the parasitic inductors in the circuit. For EMI, the decoupling capacitors together with other components, such as DC-link capacitors, busbars, connectors and parasitics, are all part of the propagation path. The voltage stress and EMI noise impact can be analyzed by simulation, as shown in Fig. 2. In the simulated chopper circuit, the DC-link capacitors, decoupling capacitors and the device module are not ideal since their parasitics impact the device stress and EMI noise spectrum significantly. The decoupling capacitor is modeled by a capacitance with 10 nH inductance and 30 mΩ resistance and the large DC link capacitor is modeled with 3900 μF capacitance, 40 nH inductance, and 100 mΩ resistance.

Since line impedance stabilization networks (LISNs) are required according to EMI noise standards [7], LISNs are placed between the converter and input source to collect EMI noises. The common-mode (CM) and differential-mode (DM) EMI noise are calculated based on their definition [8]. The double-pulse test is carried out in the simulation. Since the EMI emission and voltage stress on the device is a result of device switching, the test focuses on the turn-on and turn-off periods of the IGBT. The first pulse allows the current through the tested (bottom) switch to build up and turn off at the desired current level. With a short off period, the second pulse will turn the switch on again at practically the same current. The time-domain switching waveform can be simulated on LISNs, and the frequency-domain data can be obtained through off-line data processing [9]. In the simulation, the device is assumed to operate with 200V bus voltage and 40A load current.

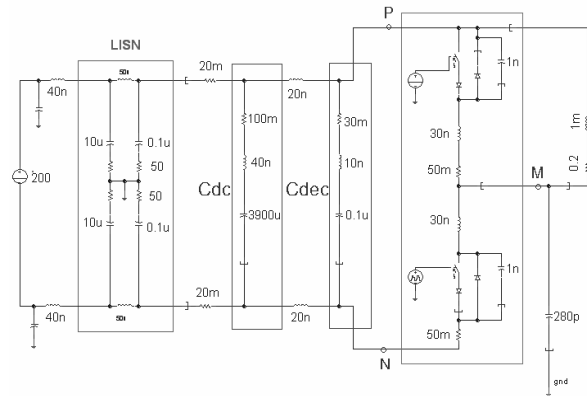


Fig. 2 Simulation of Decoupling Capacitor Effects

When changing the decoupling capacitor C_{dec} from 0 nF, to 20 nF, 50 nF, 100 nF, 500 nF, and 1 μF, the voltage stress (voltage from mid-point (M) to negative bus (E)) is reduced from 297 V to 240 V, as shown in Fig. 3. But there is no big difference (<5 V) when the capacitance is larger than 100 nF.

In DM noise spectra, as shown in Fig. 4 (a), there is a high noise peak at 12.3 MHz and no low-frequency noise peak when there are no decoupling capacitors. When adding the decoupling capacitor, the high-frequency noise is reduced significantly and the noise peak moves toward a higher frequency (17 MHz), but there is another noise peak at a lower frequency. For the high-frequency DM noise peak, since the impedance of the DC-link capacitor and busbar parasitic inductance is larger than that of the decoupling capacitor, most DM noise current flows into the decoupling capacitor. As a result, the high-frequency noise is reduced by adding the decoupling capacitor. But adding the decoupling capacitor in the circuit could cause a new resonance, which is caused by the decoupling capacitor and the parasitic inductance of busbar and the DC-link capacitor. When increasing the capacitance of the decoupling capacitor, the low-frequency noise peak is reduced and moves toward a lower frequency. Therefore, adding a decoupling capacitor to suppress voltage overshoot could cause higher EMI noise in the low-frequency range.

The CM noise spectra, as shown in Fig. 4 (b), where there is no decoupling capacitor, has one noise peak, whose frequency is the same as that of the DM noise. When adding a decoupling capacitor, the CM noise also affects the resonance between the device module and the propagation path. The high-frequency noise is pushed to a higher frequency. The noise frequency is the same as the DM noise, which shows that the resonances existing in the DM noise path induce noise in the CM path. In the simulation circuit, a capacitor is placed between device module mid-point (M) and ground to represent the parasitic capacitance between the device module and the earth ground. Any voltage change on the terminal M could induce the current to the ground, and back to the LISNs. When the device switches, the resonances make the voltage at

terminal M change. Therefore, the CM noise has the same frequency peaks.

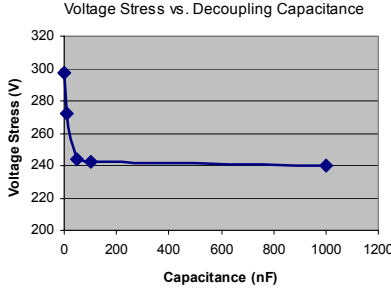


Fig. 3 Voltage Stress vs. Decoupling Capacitance

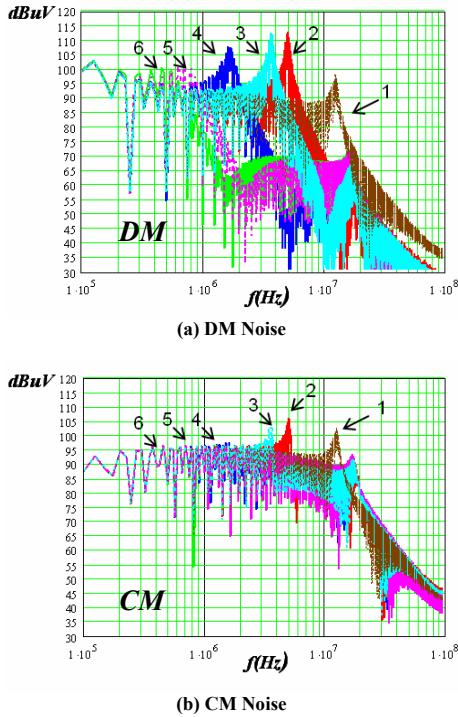


Fig. 4 Different EMI Noise Comparison When Changing Decoupling Capacitance(1: 0 nF; 2: 20nF; 3:50 nF; 4: 100 nF; 5: 500 nF; 6: 1 uF)

From simulation results, both CM and DM noise can be affected by the added decoupling capacitor. There are two noise peaks and one noise valley in the DM spectra and two noise peaks in the CM spectra. Therefore, there are at least three resonances in the circuit. When the device starts switching, for example, the bottom IGBT turns off, and the energy stored in parasitic inductances will charge the device output capacitor. When choosing a large enough decoupling capacitance, the voltage on the decoupling capacitor V_{bus} stays constant, as illustrated by the simplified model in Fig. 5. The current source in the model is a step-down pulse current, which represents the turn-off current behavior of the device.

The resonance is between the device output capacitor and the parasitic inductances of the device module and the decoupling capacitor. The overshoot voltage caused by this resonance can be approximated by Eq. 1.

$$\Delta V'_{ds}(s) = \frac{L_{bus} + L_{cap}}{L_{bus} + L_d + L_{dec}} \left[\frac{I_{switching}}{T_{off} \cdot C_{out}} \cdot \frac{1}{s(s^2 + \frac{R_d + R_{bus}}{L_{bus} + L_d + L_{dec}} \cdot s + \frac{1}{C_{out} \cdot (L_{bus} + L_d + L_{dec})})} \right] \cdot [1 - e^{-s \cdot T_{off}}] \quad (1)$$

where:

L_{bus} : the interconnection parasitic inductance between decoupling capacitor and device module, and in the simulation $L_{bus}=0$ nH

R_{bus} : the parasitic resistance of busbar and decoupling capacitor parasitic resistance

L_{dec} : the parasitic inductance of the decoupling capacitor

C_{out} : the output capacitance of the device module

R_d : the parasitic resistance of in the device module

L_d : the parasitic inductance of the device module

T_{off} : the turn-off time

When taking inverse Laplace transformation of Eq. 1, the overshoot can be calculated by Eq. 2. The time of maximum overshoot voltage is when the derivative of Eq. 2 is zero. From Eq. 2, the frequency of the noise peak and voltage overshoot is determined by the loop parasitic inductance and device output capacitance. In the simulation, when changing the decoupling capacitor, the parasitic inductance of the capacitor stays constant. From the model in Fig.5 and Eq. 2, ΔV_{ds} is the same for different decoupling capacitors.

However, in practical design, the voltage on decoupling capacitors can change in a certain range because the capacitance of the decoupling capacitor is not infinitely large. The model shown in Fig. 6 can calculate the voltage fluctuation on the decoupling capacitor. The voltage on the DC-link capacitor stays constant and the entire device is taken as a step-down pulse current source. The voltage on the decoupling capacitor ΔV_{bus} can be calculated by Eq. 3, which is similar to Eq. 2. From Eq.3, it shows that ΔV_{bus} is reduced when increasing decoupling capacitance.

$$\Delta V'_{ds}(t) = \frac{I_{switching} \cdot (L_{bus} + L_{dec})}{T_{off}} \left[1 - \frac{1}{\sqrt{1-\zeta^2}} \cdot e^{-\zeta \omega_o t} \cdot \sin(\omega_o \sqrt{1-\zeta^2} t + \psi) \right] \quad (2)$$

where

$$\zeta = \left(\frac{R_{bus} + R_d}{2} \cdot \sqrt{\frac{C_{out}}{L_d}} \right), \quad \omega_o = \sqrt{\frac{1}{(L_d + L_{bus} + L_{dec}) \cdot C_{out}}}, \quad \psi = \arccos(\zeta)$$

$$\Delta V'_{bus}(t) = \frac{I_{switching} \cdot (L_{bus1} + L_{decap})}{T_{off}} \left[1 - \frac{1}{\sqrt{1-\zeta_1^2}} \cdot e^{-\zeta_1 \omega_{o1} t} \cdot \sin(\omega_{o1} \sqrt{1-\zeta_1^2} t + \psi_1) \right] \quad (3)$$

where

$$\zeta_1 = \left(\frac{R_{bus1} + R_{dec}}{2} \cdot \sqrt{\frac{C_{dec}}{L_{dec}}} \right), \quad \omega_1 = \sqrt{\frac{1}{(L_{ddecap} + L_{bus1} + L_{dec}) \cdot C_{dec}}}$$

$$\psi = \arccos(\zeta)$$

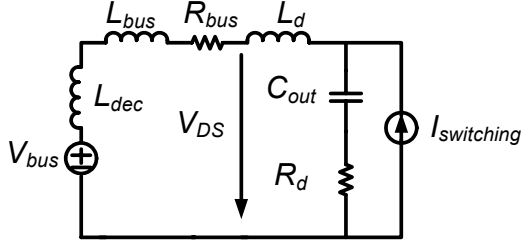


Fig. 5 Model of Voltage Overshoot and High-frequency Resonance

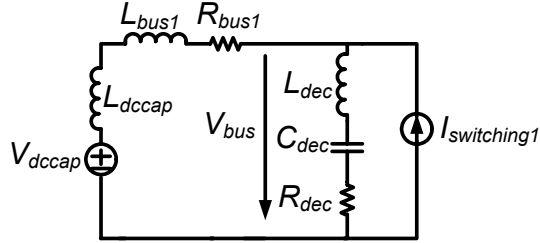


Fig. 6 Model of Voltage Overshoot and Low-frequency Resonance

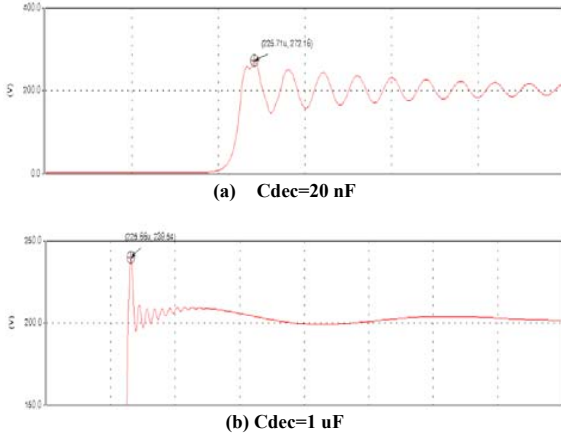


Fig. 7 Time-domain Waveforms of Terminal Voltage on Device with Different Decoupling Capacitance

The total voltage overshoot is determined by ΔV_d and ΔV_{bus} together, which can be shown as in Fig. 7 (a) and (b). When the decoupling capacitance is 20 nF, frequencies of two resonances are close, which leads to the higher voltage overshoot due to the superposition of two resonant voltages, as shown in Fig. 7 (a). When increasing the decoupling capacitance, the overshoot voltage is reduced because the ΔV_{bus} is small due to the low resonant frequency. Therefore, in a practical design, choosing ω_0 to be 10 times larger than

ω_1 , the voltage overshoot caused by the resonance between decoupling capacitor and parasitic inductance of busbar and DC-link capacitance can be neglected.

The overshoot voltage suppression could determine the minimum capacitance of the decoupling capacitor. But when considering EMI noise, larger capacitance can result in lower noise level for the low-frequency EMI noise. In practical design, low-ESL and high voltage-rating film capacitors are used as decoupling capacitors. It is not necessary to choose oversized capacitors to reduce the low-frequency EMI noise because doing so would unnecessarily increase size and cost. Nevertheless, an input EMI filter is required to attenuate low-frequency conducted EMI noise from 150 kHz up [10]. The EMI filter design is aimed at the low-frequency noise. After attenuating the low-frequency EMI noise to comply with EMI standards, the voltage transfer gain of the EMI filter will continue increasing in a certain frequency range, which could bring higher attenuation at the decoupling capacitors' first resonant frequency. Therefore, there is no need to choose too large a decoupling capacitance to attenuate the low-frequency EMI noise when the input EMI filter can be fully used.

For example, in the simulation circuit as Fig. 2, when choosing a 100 nF decoupling capacitor, the noise amplitude difference between the first peak at 1.6 MHz and the noise at 150 kHz is 5 dB μ V. If the filter has been designed to attenuate the noise at 150 kHz to pass the standards, the filter needs to have 5 dB more attenuation to suppress the noise peak at 1.6 MHz. In a one-stage filter, when it can be used to attenuate noise at 150 kHz, it can have 40 dB more attenuation at 1.6 MHz, which is enough for attenuating the noise. As a result, the 100 nF decoupling capacitor can satisfy the suppression of overshoot voltage while not requiring a bigger EMI filter. Theoretically, from a filter design point of view, the attenuation can be higher and higher when frequency increases. But this is not true in reality because of the parasitics of the filter itself and the property of magnetic core materials used for filter inductor changes at high frequencies. As a result, the filter designed for the low-frequency attenuation can magnify the EMI noise. Research has been conducted to eliminate the effect of filter parasitics [11]. Though adding a decoupling capacitor can reduce the high-frequency noise, it still causes another noise peak at the high frequency. Compared to the low-frequency noise peak, the high-frequency noise is more difficult to attenuate with the input EMI filter. One way to reduce the high-frequency noise peak is to choose a low-ESL capacitor and use devices with lower lead inductance. In [11] a method to cancel the parasitic inductance in the capacitor was proposed, which provides good results for lowering the high-frequency noise peak.

III. EMI FILTERING STRATEGY FOR HIGH-FREQUENCY NOISE

As discussed above, decoupling capacitors are introduced for the device safe operation. In order to further reduce the overshoot voltage, parasitic inductance of the decoupling capacitor and the device module should be minimized. In DM

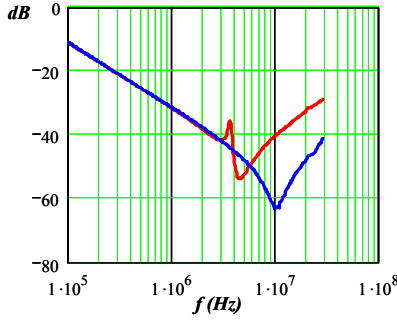


Fig. 8 Voltage Transfer Gains With and Without ESL Cancellation

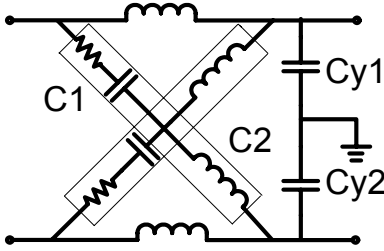


Fig. 9 High-frequency Filter Structure

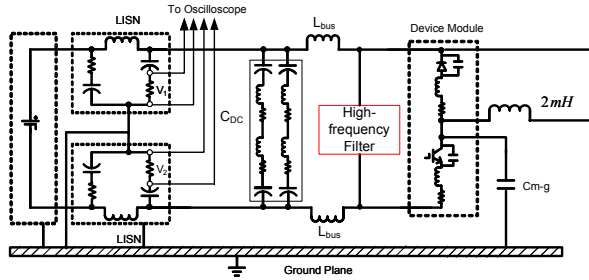


Fig. 10 Chopper Circuit Testbed for High-frequency Filter

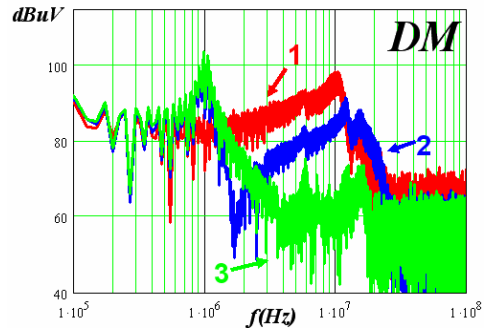
noise spectra as shown in Fig. 4 (a), the decoupling capacitor attenuates the noise after the first noise peak, therefore behaving as a DM noise filter. There is a DM noise valley because of self-resonance of the decoupling capacitor and its parasitic inductor. When frequency increases, the decoupling capacitor behaves more as an inductor. In order to maximize the DM filtering effect of the decoupling capacitor, reducing the capacitors' ESL is a straightforward method. In [11], an effective way to minimize the ESL in capacitors was proposed. The principle can be described as follows: when two capacitors are in parallel, by designing the connecting PCB trace inductance and connection way, the ESL of the capacitors can be eliminated from the network point of view. In the experiment, two 100nF film capacitors are used as the decoupling capacitors. Fig. 8 shows the voltage transfer gains with and without ESL cancellation. It can be seen that the resonant frequency is pushed from 4 MHz to 10 MHz. With

the cancellation, the two parallel decoupling capacitors have better high-frequency characteristics.

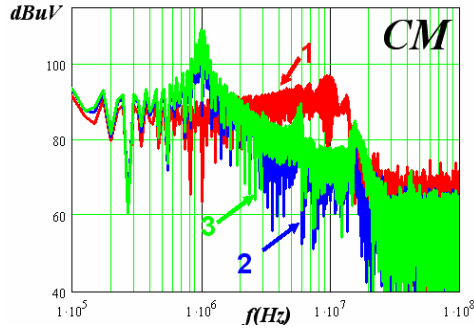
Another important function of the decoupling capacitors is to eliminate inductance unbalance of the busbar and interconnection parasitics. The possibility of DM noise transferring to CM noise can be reduced [12]. As a result, the CM noise filtering strategy can be more effective. Furthermore, it is difficult to attenuate EMI noise because of the non-ideal characteristics of the input EMI filter and complicate noise propagation path. Therefore, attenuating EMI noise at the noise generation point, i.e., close to device switching, is desirable by providing a return path for EMI noise and containing EMI noise to the noise source side. In addition, the filtering stress of the input EMI filter can be reduced, especially for the high-frequency noise.

As mentioned above, the decoupling capacitor is adopted as the DM noise filter on the noise source side. The simplest structure of the CM noise filter is to add capacitors between the bus and ground. With the balance effect of the decoupling capacitor, two 3 nF ceramic Y capacitors can be added at the device terminals. The proposed filter structure is shown in Fig. 9. The entire filter is composed of three capacitors and PCB traces. The high-frequency filter is tested in the testbed as shown in Fig. 10.

Fig. 11 (a) and (b) show the EMI noise comparison. With the high-frequency filter, the DM noise from 3 MHz and up is much lower than without filter and without ESL cancellation as shown in Fig. 11 (a). Without the decoupling capacitor, there is a noise peak at 10 MHz. When adding decoupling capacitors with parallel structure, the noise peak is pushed to 12 MHz. Both of these noise peaks are very difficult to attenuate by the input EMI filter. With the ESL cancellation, the DM noise peaks are reduced by 30 dB μ V. Therefore, the stress of the input filter to attenuate the high-frequency EMI noise is reduced significantly. As discussed above, adding decoupling capacitors brings the low-frequency resonance. It is about 10dB μ V higher at 1MHz than at 150 kHz. For one-stage or two-stage input EMI filter, the attenuation at 1MHz will be around 40 dB or more, which can attenuate the noise peak efficiently.



(a) DM Noise

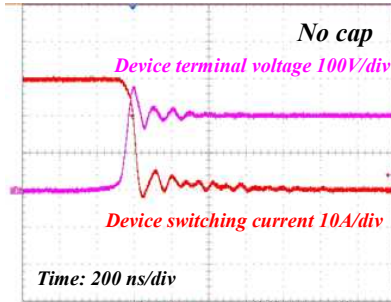


(b) CM Noise

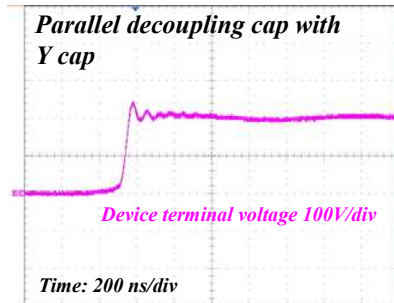
Fig. 11 Comparisons of DM and CM Noise.
(Trace 1: without high-frequency filter; Trace 2: high-frequency capacitor with two capacitors in parallel and Y capacitors; Trace 3: proposed high-frequency filter)

For CM noise, adding Y capacitors, for both cases with and without ESL cancellation, can reduce CM noise from 3 MHz and up. The noise peak at 10 MHz is reduced by 18 dBμV. Therefore, the proposed high-frequency filter can reduce both CM and DM noise.

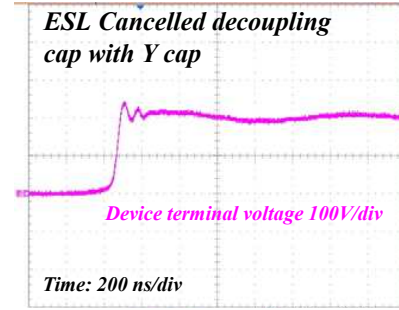
With decoupling capacitors, the voltage overshoot can be reduced by 40 V, shown in Fig. 12. With or without ESL cancellation, decoupling capacitors have the similar voltage stress suppression.



(a) No High-frequency Filter



(b) High-frequency Filter - Parallel Decoupling Capacitors with Y Capacitors



(c) Proposed High-frequency Filter

Fig. 12 Voltage Overshoot Comparison

IV. INTEGRATED HIGH-FREQUENCY EMI FILTER IN POWER ELECTRONICS MODULES

The high-frequency filter can effectively reduce EMI noise and device voltage stress. It is different from the traditional EMI filter in that it only includes three capacitors. Because there is no inductor used in the filter, the size of the filter is much smaller than the traditional EMI filter. This provides the possibility to integrate the high-frequency filter into the device module. In the IPEM design [6], the 400 nF decoupling capacitor was integrated. It also demonstrates the function of suppressing the device voltage overshoot. Two Y capacitors need to be integrated into the IPEM module. Compared with the decoupling capacitor, the capacitance of two Y capacitors is much smaller. Commercial ceramic capacitors with surface-mount package can be used to connect the two buses to direct-bonding-copper (DBC), which is the reference ground of the device module. Note that the device parasitic inductance can be reduced significantly by the IPEM packaging technology, as shown in Fig. 13. The magnitude of the resonance caused by the device output capacitance and parasitic inductance of the device packaging and the decoupling capacitance can be reduced.

Fig. 14 shows the simulation results of the IPEM used in the chopper circuit. The Y capacitors do not affect the DM noise significantly in the conducted EMI range. However, the Y capacitors help attenuate the CM noise from 1 MHz and up. Therefore, the integrated high-frequency filter can improve IPEM EMI performance. Note that the parasitic inductance of the Y capacitor branch should be minimized. Otherwise, the attenuation of the Y capacitor will be reduced by the resonance in the Y capacitor branch. Theoretically, a larger Y capacitor can further reduce CM noise on the input side since it provides a low impedance CM noise path. However, it still cannot replace the input EMI filter because the noise propagation path outside of the device module is complicated and can cause other noise peaks, as shown in Fig. 4 (b). Generally, the high-frequency filter can help reduce EMI noise in the converter. The effectiveness of the filter will vary in different converters.

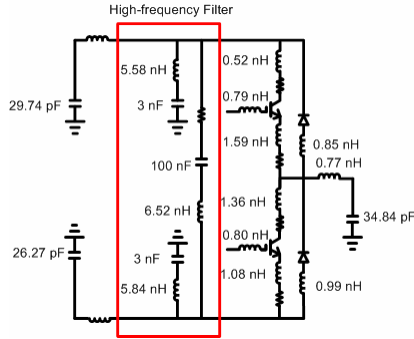


Fig. 13 IPEM Structure

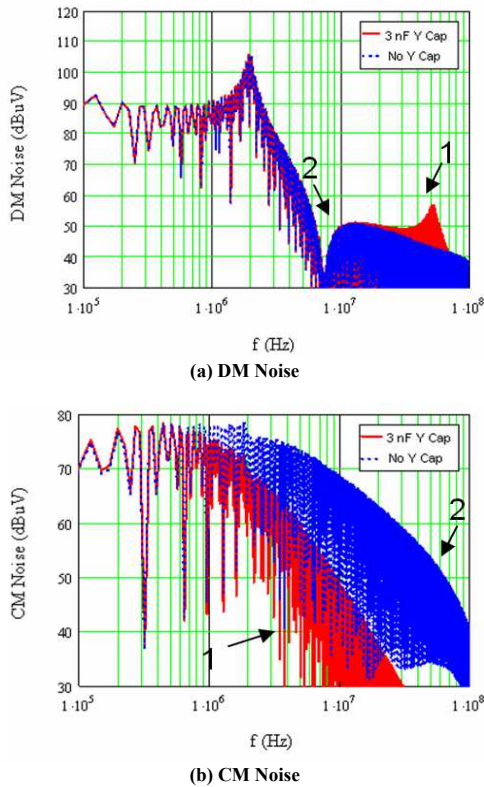


Fig. 14 EMI Noise Comparison between Cases with/without Y Capacitor

V. CONCLUSION

In this paper, the impacts of the decoupling capacitors on voltage overshoot and EMI noise are analyzed. Adding the decoupling capacitors can effectively reduce the voltage stress of the device. They also have great impact on CM and DM EMI noises both in low and high frequency ranges. The analytical method is presented to select decoupling capacitors considering both voltage overshoot and EMI noise. Since the switching behavior of devices is the noise source, an effective noise filtering scheme is to provide a noise path to contain the

EMI noise at the noise source side, especially for the high-frequency EMI noise. A simple high-frequency EMI filter, which includes the decoupling capacitors, two Y capacitors, and PCB traces, is proposed. The experimental results show that the CM and DM noise can be attenuated significantly from 3 MHz and up. This filter structure can be integrated in the device module, which is demonstrated in the IPEM design. The simulation results verify the function of the high-frequency filter, which can reduce the filtering stress of the input EMI filter for the high-frequency noise. The EMI performance of the device module can be improved by this integrated local high-frequency filter.

ACKNOWLEDGMENT

This work was supported primarily by the Engineering Research Center Program of the National Science Foundation under NSF Award Number EEC-9731677 and the CPES Industry Partnership Program.

REFERENCES

- [1] H.J. Beukes, J.H.R. Enslin, R. Spee, "Busbar design considerations for high power IGBT converters," In IEEE Proc. on *PESC '97*, vol. 2, pp. 847 – 853
- [2] W. Teulings, J. L. Schanen, J. Roudet, "MOSFET switching behaviour under influence of PCB stray inductance," In IEEE Proc. on *IAS'06*, vol. 3, pp.1449 – 1453
- [3] F. Z. Peng, G.-J. Su; L. M. Tolbert, "A passive soft-switching snubber for PWM inverters," IEEE Trans. on *Power Electronics*, vol. 19, Issue 2, pp. 363 – 370, 2004
- [4] F. Blaabjerg, A. Consoli, J. A. Ferreira, J. D. van Wyk, "The future of electronic power processing and conversion," IEEE Trans. on *Industry Applications*, vol. 41, Issue 1, pp. 3 – 8, 2005
- [5] Z. X. Liang, F. C. Lee, J. D. van Wyk, D. Boroyevich, D. Scott, J. Chen, B. Lu, Y. Pang, "Integrated packaging of a 1 kW switching module using planar interconnect on embedded power chips technology," In IEEE Proc. on *APEC '03*, vol. 1, pp. 42 – 47
- [6] Z. X. Liang; J. D. van Wyk, "Functional integration in active IPEM by using a planar integration technology," In IEEE Proc. *APEC'05*, vol. 1, pp. 375 – 381
- [7] CISPR11: Industrial, scientific and medical (ISM) radio-frequency equipment - Electromagnetic disturbance characteristics - Limits and methods of measurement, International Special Committee on Radio Interference, 2004
- [8] C. Paul, "Introduction to Electromagnetic compatibility," Wiley, 1992
- [9] Q. Liu, W. Shen, F. Wang, D. Boroyevich, V. Stefanovic and M. Arpilliere, "Experimental evaluation of IGBTs for characterizing and modeling conducted EMI emission in PWM inverters," in Proc. IEEE *PESC'03*, vol. 4, pp. 1951 – 1956
- [10] F. Y. Shih, D. Y. Chen, Y. P. Wu, Y. T. Chen, "A procedure for designing EMI filters for AC line applications," IEEE Trans. on *Power Electronics*, vol. 11, Issue 1, Jan. 1996, pp. 170 – 181
- [11] S. Wang; F. C. Lee, W. G. Odendaal, J. D. van Wyk, "Improvement of EMI filter performance with parasitic coupling cancellation," IEEE Trans. on *Power Electronics*, vol. 20, Issue 5, pp. 1221 – 1228, 2005
- [12] S. Wang, "Characterization and Cancellation of High-Frequency Parasitics for EMI filters and Noise Separators in Power Electronics Applications," Ph. D Dissertation, Virginia Tech, 2005
- [13] G. L. Skibinski, R. J. Kerkman and D. Schlegel, "EMI emissions of modern PWM AC drives," In IEEE Industry Applications Magazine, vol. 5, Issue: 6, pp. 47 – 80, 1999